

## **Effect of Hemoglobin Adsorption on Apparent Capacitance Density of Platinum Disk Nanoelectrode**

*Chengyin Wang\**, *Yujing Chen*, *Xiaoya Hu\**, *Rong Guo*

Department of Chemistry and Chemical Engineering, Yangzhou University, Yangzhou 225002, China

\*E-mail: [yzswcy@yzcn.net](mailto:yzswcy@yzcn.net) (C. Wang) and [xyhu@yzu.edu.cn](mailto:xyhu@yzu.edu.cn) (X. Hu)

*Received:* 14 April 2006 / *Accepted:* 21 June 2006 / *Published:* 22 June 2006

---

A platinum disk nanoelectrode was prepared by sealing a platinum wire etched electrochemically in epoxy resin. Its apparent capacitance density (ACD) increased exponentially with its decreasing geometrical area. The adsorption of hemoglobin molecules on the nanoelectrode resulted in the decrease of its effective area, leading to a significant change of its apparent capacitance. The hemoglobin molecules adsorbed could be estimated according to the dimension of single hemoglobin molecule. Thus, a new electrochemical method for highly sensitive sensing of some electroinactive molecules could further be developed.

---

**Keywords:** platinum, hemoglobin, nanoelectrode, apparent capacitance density

### **1. INTRODUCTION**

With development of analytical nanotechnology, detections of less and less amount of analytes were achieved by a variety of analytical methods, and the detection limits were improved step by step, even single-molecule detection had been realized [1,2]. Detection of single molecules labeled with ~100-fluorescein fluorophores was first reported by Hirschfeld in 1976 using laser-induced fluorescence [3]. Shera et al began their quest to detect single-fluorophore molecules in flow in 1983 and progressed until they detected them in 1990 [4]. Bard et al realized the detection of single molecule in 1995 with a nanoelectrode by the electrochemical method [5], and in 1997 they subsequently explored the detection of single electron-transfer events at nanometer electrodes known as the electrochemical "Coulomb Staircase" [6]. Collison et al have explored single molecule detection at electrodes by electrochemical method, and single reaction events of reactants generated at electrodes can be observed [7]. White et al have detected zeptomole of electroactive species adsorbed at a platinum electrode of nanometer dimensions by the voltammetric method [8]. In the case, voltammetric peaks corresponding to oxidation of as few as ~ 7000 adsorbed redox molecules (~ 11 zmol) at individual

nanoelectrodes are reported, allowing precise measurement of electrode areas as small as  $\sim 10^{-10}$  cm<sup>2</sup>. Duyne et al investigated the localized surface plasmon resonance  $\lambda_{max}$  response of individual Ag nanoparticles [9]. They found the adsorption of fewer than 60000 1-hexadecanethiol molecules ( $\sim 100$  zeptomole) on single Ag nanoparticles resulted in a localized surface plasmon resonance shift of 40.7 nm. Matsuya et al prepared a core-shell-type fluorescent nanosphere covalently conjugated with antibody for zeptomole detection of protein in time-resolved fluorometric immunoassay [10]. Dore et al reported the specific detection of a few hundred molecules of genetic material using a fluorescent polythiophene biosensor based on simple electrostatic interactions between a cationic polymeric optical transducer and the negatively charged nucleic acid target [11]. However, up to now, there has been no paper reported about the sensitivity of hemoglobin molecules at a platinum disk nanoelectrode based on a response of its apparent capacitance.

In the present report, we describe the characterization of platinum disk electrodes of nanometer dimensions (radius 7.6-380 nm) prepared by sealing a platinum wire etched electrochemically in epoxy resin. The goals of these experiments are to develop a novel electrochemical method for highly sensing of electroinactive molecules adsorbed on the individual nanoelectrode surface using hemoglobin as an example, steady-state voltammetric limiting currents ( $I_{lim}$ ) in determining the electrode area and its apparent capacitance density (ACD).

## 2. EXPERIMENTAL PART

### 2.1 Apparatus

Cyclic voltammetry (CVs) was carried out with CHI660A electrochemical workstation (Chenhua Instrument Limited Company, Shanghai) in conjunction with a computer. The high-sensitivity preamplifier (1 pA/V) of the potentiostat was used in all experiments. A three-electrode system was employed. A platinum disk nanoelectrode was used as a working electrode. A saturated calomel electrode and a platinum plate were served as the reference and auxiliary electrode, respectively. XL-30 ESEM scanning Electron Microscope (Philips, Holland) was used for the surface characterization of the etched electrodes.

### 2.2 Materials

Micro platinum wires with a radius of 10  $\mu$ m were purchased from Shanghai Chemicals Co. (Shanghai, China). High pureness of bovine heart hemoglobin (crystal grade) was obtained from the Institute of Shanghai Biochemistry (Shanghai, China). HAc-NaAc buffer solution (pH 5.5, 0.20 mol/L) was used to prepare 0.1 mmol/L hemoglobin solution. All biochemical reagents and solutions were stored in refrigerator below 5 °C, and the experiments were carried out at 26 °C. The other reagents

were analytical grade. Doubly distilled water was obtained by purification through a Millipore Water System and was used throughout.

### 2.3 Fabrication of the platinum disk nanoelectrode

According to previous literature [12], a platinum wire of about 10 mm in length was combined with one end of a copper wire by spot welding. After being rinsed with ethanol and water, the platinum wire was immersed in an etching solution (saturated sodium nitrite aqueous solution). An AC voltage was applied for the electrochemical etching between the platinum wire and a platinum foil electrode (Figure 1). The etching process was not completed until the current dropped to zero, indicating the wire was no longer in contact with the solution, and then the wire was carefully rinsed with water to remove residual  $\text{NaNO}_2$ . The SEM image of the etched platinum wire is shown in Figure 2.

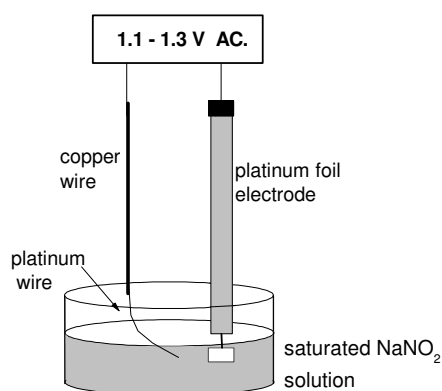


**Figure 1.** The schematics of the etching of platinum wire.

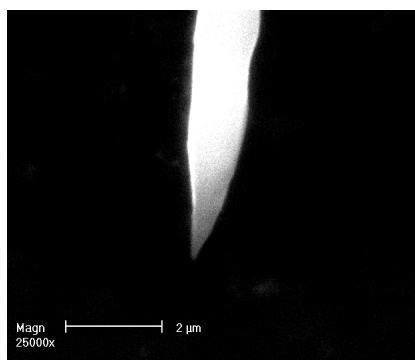


**Figure 2.** Scanning electron microscopy image of the etched nanoelectrode

The etched platinum wire was sealed by the epoxy resin (Jiangnan Adheslve CO., LTD, Changshu, China) in a plastic tube (2 mm in radius, 5 cm in length). The configuration of the platinum wire

microelectrode is illustrated in Figure 3. The unfinished electrode was vertically placed and dried in air at room temperature for 24 hours. Before we polished electrode, a line was drawn to mark the position of platinum wire tip in the tube so as to facilitate the electrode polish treatment. The polish treatment of the electrode with rough and fine sandpapers respectively did not stop till to the tube end approached the marked line. And then it was polished with fine alumina slurry (particle size:  $0.03\ \mu\text{m}$ ) on a piece of silk. In the process of electrode polish, the electrode as a working electrode, a platinum wire as an auxiliary electrode and a saturated calomel electrode as a reference electrode, were continually immersed in  $0.01\ \text{mol/L}\ \text{K}_3\text{Fe}(\text{CN})_6$  solution containing  $0.5\ \text{mol/L}\ \text{KCl}$  to record the response using steady-state cyclic voltammetry. When a well-defined sigmoidal wave with picoamps current was obtained, the platinum disk ultramicroelectrode was prepared.

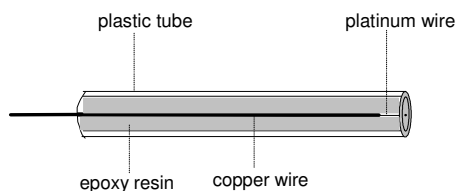


**Figure 3.** The schematics of the platinum disk nanoelectrode.

#### 2.4 The adsorption of hemoglobin at the platinum disk nanoelectrode

The effective area of the bare platinum disc electrode was first determined by measuring limiting plateau current in  $0.01\ \text{mol/L}\ \text{K}_3\text{Fe}(\text{CN})_6$  solution containing  $0.5\ \text{mol/L}\ \text{KCl}$ . Then, the proposed electrode was immersed in  $0.1\ \text{mmol/L}$  hemoglobin solution containing  $0.20\ \text{mol/L}$  acetate buffer for certain times. Finally, the electrode adsorbed with hemoglobin was immersed again in  $0.01\ \text{mol/L}\ \text{K}_3\text{Fe}(\text{CN})_6$  solution containing  $0.5\ \text{mol/L}\ \text{KCl}$  for determination of effective electrode area. The amount of adsorbed hemoglobin could be calculated based on the electrode area occupied by hemoglobin molecules (the decrease amounts of effective electrode areas after adsorption of hemoglobin) and the size of single hemoglobin molecule. The apparent capacitance was measured by cyclic voltammetry between  $-0.6$  and  $1.0\ \text{V}$  in  $0.2\ \text{mol/L}$  acetate buffer (pH, 5.5) and the charging currents at  $0.1\ \text{V}$  were recorded. The slope of a plot (the charging currents versus scan rates) was the value of apparent capacitance

### 3. RESULTS AND DISCUSSION

#### 3.1 Effect of the etching voltage

The employed voltage for the electrochemical etching process could affect the shape of the etched platinum wire tip. When the voltage is higher than  $1.3\ \text{V}$ , the etching process within several seconds is

too fast to obtain a regular acuminate shape. When the voltage is in the range of 1.1 - 1.3 V, the regular tip is obtained. The SEM image of the etched platinum wire is shown in Figure 2. When the voltage is less than 1.1 V, more than 1 hour is spent. So the etching voltage of 1.1 - 1.3 V was chosen. Additionally, The Pt wire was etched to a sharp point by placing the wire in a saturated sodium nitrite solution. The sharpest point of the etched Pt wire was obtained when the end of Pt wire was inclined to be submerged in the electrochemical etching solution at a 30 - 60° angle rather than submerged perpendicularly (Figure 1).

### 3.2 Effect of the concentration of sodium nitrite solution

The concentration of the sodium nitrite solution also plays an important role in the shape of the etched platinum wire tip and the etching time. When the concentration of sodium nitrite solution is less than 1 mol/L, the etching rate is slow; the surface of the etched platinum wire tip is rough, and the tip is easily broken. By the increasing the concentration of the sodium nitrite solution, the etching is quicker, and the tip becomes sharp enough. Therefore a saturated sodium nitrite solution was the best choice for etching platinum wire.

### 3.3 Determination of the geometric area of the platinum disk nanoelectrode

In characterization studies of ultramicroelectrodes (UMEs), steady-state voltammetry (SSV) can provide an estimate of the exposed electroactive radius of the nanoelectrode. Figure 4 shows voltammograms of two platinum wire electrodes in 0.01 mol/L  $\text{K}_3\text{Fe}(\text{CN})_6$  with a supporting electrolyte of 0.5 mol/L KCl. Assuming that the electrode is a d shape, the effective radii  $r_{\text{eff}}$  of these electrodes can be determined from the limiting plateau currents ( $I_{\text{lim}}$ ) according to the following equation [21]:

$$I_{\text{lim}} = 4nFDrc \quad (1)$$

Where  $n$  is the number of electrons transferred during the electrochemical process,  $F$  is faraday's constant,  $D$  and  $c$  are the diffusion coefficient and concentration of the electroactive species. By using the known value of the diffusion coefficient of ferricyanide,  $7.2 \times 10^{-6} \text{ cm}^2 \text{ s}^{-1}$  [22], the effective radii of the electrodes in Figure 4 is calculated as 7.6 nm, 30 nm, 75 nm, 134 nm and 380 nm, respectively. White has pointed out that while the initial scan yielded a near-ideal response in  $\text{K}_4\text{Fe}(\text{CN})_6$  solution with a platinum nanoelectrode fabricated by electrophoretic paint method, the reverse and subsequent scans were quite poorly defined with the current decreasing, which was explained as the adsorption of  $\text{Fe}(\text{CN})_6^{4-}$  [23]. However, in this paper we used  $\text{K}_3\text{Fe}(\text{CN})_6$  or  $\text{K}_4\text{Fe}(\text{CN})_6$  as the probe for determining the effective area of platinum disk nanoelectrode, and achieved good reproducibility and accuracy with the relative standard deviation of 4.9 %. Figure 5 shows the cyclic voltammograms of the 42 nm-radius

platinum nanoelectrode in  $K_4Fe(CN)_6$  solution. Solid line is the first scan, and dash line is curve after 10 cycle scans.

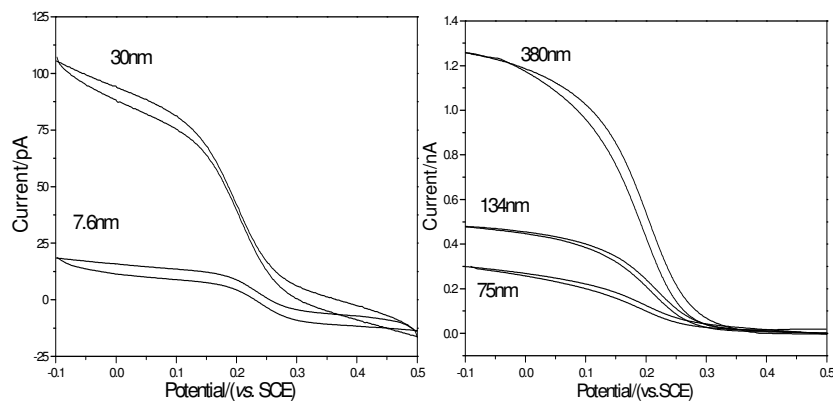


**Figure 4.** The steady-state voltammograms of the platinum disk nanoelectrode in 0.5 mol/L KCl containing 0.01 mol/L  $K_3Fe(CN)_6$ . The effective radii of the nanoelectrodes were calculated from the limited currents as 7.6 nm, 30 nm, 75 nm, 134 nm and 380 nm, respectively. A saturated calomel electrode was served as the reference electrode and a platinum plate was served as the auxiliary electrode. The scan rate was 5 mV/s.

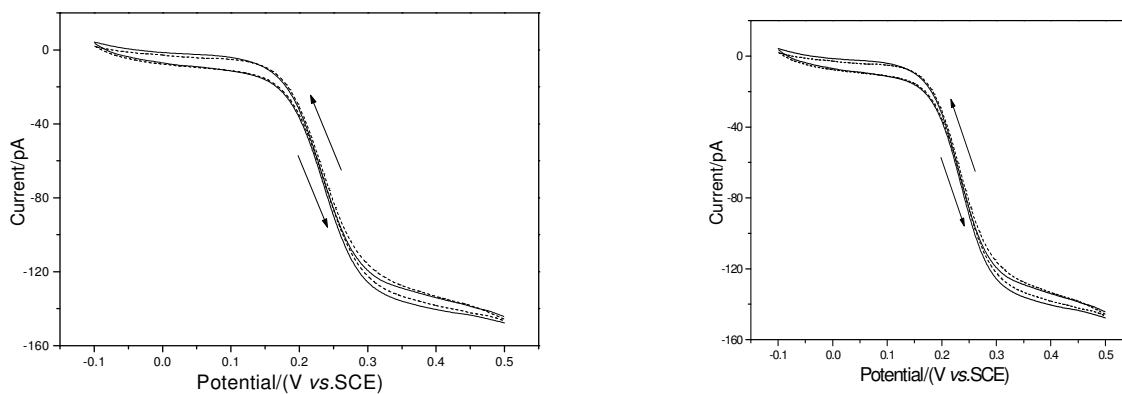


**Figure 5.** The steady-state voltammograms of 0.01 mol/L  $K_4Fe(CN)_6$  in 0.5 mol/L KCl using 42 nm-radius platinum disk nanoelectrodes. Solid line was the first scan, and dash line was the curve after 10 cycle scans.

### 3.5 Determination of the real surface areas of the Platinum disk nanoelectrode

The real surface areas of the platinum electrode can be determined by cyclic voltammetry using the hydrogen adsorption peaks in 0.5 mol/L  $H_2SO_4$  [16] or 0.2 mol/L acetate buffer solution[17]. Figure 6

shows the cyclic voltammogram of the 134 nm-radius platinum disk nanoelectrode from -0.6 V to 1.0 V in the 0.2 mol/L acetate buffer (pH 5.5, 26 °C). The real surface area of the platinum disk nanoelectrode ( $S_r$ ) could be calculated as follows [24]:

$$S_r = \frac{Q_m}{ed_m} \quad (2)$$

where  $S_r$  is the real surface area of the platinum disk nanoelectrode,  $Q_m$  is the hydrogen adsorption charge associated with the formation of a monolayer,  $e$  is the electron charge, and  $d_m$  is the density of the surface metal atom. The value of  $d_m$  can be calculated using the Anderson criterion [25], which proposes that for aged polycrystalline surfaces, the lower Miller index planes (100), (110), (111) predominate, in a proportion of 33 % for each one. In this case,  $d_m$  is  $1.3 \times 10^{15} \text{ cm}^{-2}$  [26]. So,  $e \times d_m = (1.602 \times 10^{-19} \text{ C}) \times (1.3 \times 10^{15} \text{ cm}^{-2}) = 208 \text{ } \mu\text{C}/\text{cm}^2$ .

The real surface area is always larger than the geometric area, and the roughness factor  $\rho$  is the ratio of the two [16]:

$$\rho = S_r / S_g \quad (3)$$

where  $S_r$  and  $S_g$  are the real surface area and the geometric area, respectively. From equation (2) and (3), the roughness factor  $\rho$  of 380 nm, 134 nm and 75 nm-radii platinum disk nanoelectrode resulted in 2.23, 1.31 and 1.10, respectively in the 0.2 mol/L acetate buffer solution. These results were consistent with those resulted from 0.5 mol/L  $\text{H}_2\text{SO}_4$  solution. The roughness factor  $\rho$  will approach 1 when the radius of the platinum disk nanoelectrode was close to 30 nm. So the adsorption of hemoglobin took place just on the plane of platinum surface rather than on the roughness surface.

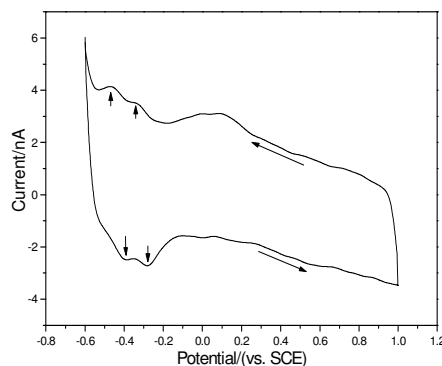


**Figure 6.** The cyclic voltammograms of the platinum disk nanoelectrode with the effective radius of 134 nm in the 0.2 mol/L acetate buffer solution, pH 5.5, at 26 °C. The scan rate was 10 V/s. The arrowheads show the hydrogen adsorption and desorption peaks.

The platinum disk nanoelectrode fabricated by using the electrophoretic paint suffered from large capacitive current associated with the polymer coating [8]. So it was difficult to observe the adsorption peak when the radius of the platinum disk nanoelectrode was smaller than 170 nm, even based on using Apiezon wax. But in our experiments, hydrogen adsorption peaks of 134 nm platinum disk nanoelectrode fabricated by sealing coat of epoxy resin could be observed clearly (Figure 6). However, the hydrogen absorption current approached to the capacitive current when the radius of platinum disk nanoelectrode was close to 30 nm, which disturbed accurate determination of electric charge of hydrogen absorption.

### 3.6 Estimation of the Amount of hemoglobin adsorbed

The amount of the hemoglobin adsorbed at the platinum disk nanoelectrode surfaces can be calculated based on below equation:

$$n_h = \frac{A_0 - A_a}{A_h} \quad (4)$$

where  $n_h$  is the molecular number of hemoglobin adsorbed at the electrode surface.  $A_0$  and  $A_a$  are the effective areas of the bare electrode and the electrodes adsorbed with hemoglobin respectively.  $A_h$  is the area occupied by single hemoglobin molecule. Each hemoglobin molecule is considered as a similar ball with the diameter of 5.5 nm [27], so,  $A_h$  is 23.8 nm<sup>2</sup>.  $A_0$  and  $A_a$  could be determined from the steady-state diffusion-limited current of the platinum disk nanoelectrode in 0.01 mol/L K<sub>3</sub>Fe(CN)<sub>6</sub> solution containing 0.5 mol/L KCl. Figure 7 shows the cyclic voltammograms of the platinum disk nanoelectrode with the radii of 96 nm (A) and 24 nm (B) which adsorbed with different amounts of hemoglobin within different times. The limited currents decreased with the increase of hemoglobin adsorbed. The amount of the hemoglobin adsorbed at the platinum disk nanoelectrode was calculated and shown in Table 1.

**Table 1.** The number of hemoglobin molecules adsorbed at the platinum disk nanoelectrodes

Electrode effective radius (nm)	Absorption time in hemoglobin solution (min)	The amount of adsorbed hemoglobin molecules	The increments of adsorbed hemoglobin molecules compared with previous adsorption
96	10	195	195
96	30	963	768
96	60	1155	192
96	120	1218	63
24	10	35	35
24	30	68	33

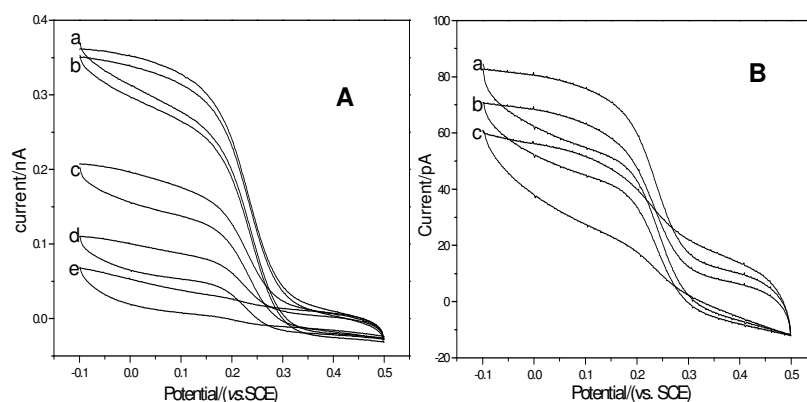


**Figure 7.** The steady-state voltammograms of 0.01 mol/L  $K_3Fe(CN)_6$  in 0.5 mol/L KCl using the platinum disk nanoelectrodes. (A) The apparent radius was 96 nm, a - e were the bare electrode immersed in 0.1 mmol/L hemoglobin solution for 0, 10, 30, 60 and 120 min respectively. (B) The effective radius was 24 nm, A and B were the bare electrode immersed in 0.1mmol/L hemoglobin solution for 0, 10 and 30 min respectively. Scan rate: 5 mV/s.

### 3.7 Effect of hemoglobin adsorbed on the apparent capacitance of the platinum disk nanoelectrode

The apparent capacitance of the electrode was measured by cyclic voltammetry between - 0.6 and 1.0 V in 0.2 mol/L acetate buffer (pH, 5.5) and the charging currents at 0.1 V were recorded. The slope of a plot (the charging currents versus scan rates) was the value of apparent capacitance [18-20]. The region of cyclic voltammetric curve from 0 to 0.3 V is known as the double-layer region where the dominating current is the capacitive current with the smallest Faraday current. The ACDs of the different size electrodes before and after saturated adsorption of hemoglobin were shown in Figure 8 and Table 2, and it was surprising that the ACDs grew exponentially with the decrease of the nanoelectrode areas. The maximum was  $7.6 \times 10^4 \mu F/cm^2$  when the effective radius of platinum disk nanoelectrode was 7.6 nm. The equation (5) was obtained by Non-linear Curve Fit as follows:

$$C_d = 1 + 616.8e^{-r/12.1} + 2208.6e^{-r/4.6} \quad (5)$$

Where  $C_d$  is the apparent capacitance density with the unit of  $\times 10^2 \mu F/cm^2$ ,  $r$  is the effective radius of platinum disk nanoelectrode. According to Table 2, it is clear that the ACD of the platinum disk nanoelectrode adsorbed with hemoglobin was smaller than that of the bare electrodes. This relationship was probably caused by the edge effect of the nanoelectrode. The decrease percent of ACD after adsorption of hemoglobin increased when the size of the platinum disk nanoelectrode decreased, which it facilitates the calculation of fewer molecules. The ACDs of the electrodes adsorbed with hemoglobin were smaller than those of the bare electrodes, owing to the ACD in inverse proportion to the thickness of adsorbed molecules according to below equation (6):

$$C_d = \frac{\epsilon_r \epsilon_0}{d} \tag{6}$$

where  $C_d$  is the ACD,  $\epsilon_r$  is the permittivity of molecules adsorbed,  $\epsilon_0$  is the permittivity of the free space,  $d$  is the thickness of molecules adsorbed. According to above equations (1, 4 and 5), the relation between the ACD change and the amount of adsorbed hemoglobin could be deduced as follows:

$$C_d = 1 + 616.8 \exp\left(-\frac{1}{12.1} \sqrt{r_0 - \frac{nA_h}{\pi}}\right) + 2208.6 \exp\left(-\frac{1}{4.6} \sqrt{r_0 - \frac{nA_h}{\pi}}\right) \tag{7}$$

Where  $C_d$  is the apparent capacitance density with the unit of  $\times 10^2 \mu\text{F}/\text{cm}^2$ ;  $r_0$  is the effective radius of bare platinum disk nanoelectrode;  $n$  is the amount of adsorbed hemoglobin;  $A_h$  is the area occupied with single hemoglobin molecule.

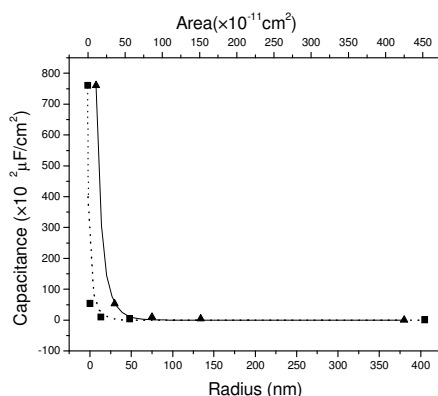


**Figure 8.** The apparent capacitance density as a functional of (a) the radius of the electrodes (triangle), (b) the area of the electrodes (square).

**Table 2.** The apparent capacitance density (ACD) of the platinum disk nanoelectrodes before and after adsorption of hemoglobin molecules

Effective radius (nm)	ACD ( $\times 10^2 \mu\text{F}/\text{cm}^2$ )	ACD after saturated adsorption of hemoglobin ( $\times 10^2 \mu\text{F}/\text{cm}^2$ )	Decrease amounts of ACD after saturated adsorption of hemoglobin ( $\times 10^2 \mu\text{F}/\text{cm}^2$ )	Changing rate of the apparent capacitance after adsorption of hemoglobin (%)
380	1.00	0.96	-0.04	-4.61
134	4.27	4.00	-0.27	-6.22
75	9.55	8.87	-0.68	-7.10
30	53.70	43.40	-10.30	-19.1
7.6	760.75	-	-	-

#### 4. CONCLUSIONS

In this paper, a platinum disk nanoelectrode was prepared by sealing a platinum wire etched electrochemically in epoxy resin for the adsorption of hemoglobin molecule in 0.2 mol/L acetate buffer. Its apparent capacitance density (ACD) increased exponentially with its decreasing geometrical area. The adsorption of hemoglobin molecules on the nanoelectrode resulted in the decrease of its effective area, leading to a significant change of its apparent capacitance. The hemoglobin molecules adsorbed could be estimated according to the dimension of single hemoglobin molecule. The determination of the apparent capacitance was comparatively easy and simple. Thus, a new electrochemical method for highly sensitive sensing of some electroinactive molecules, even single molecule, could further be developed.

#### ACKNOWLEDGEMENTS

This work was supported by the National Natural Science Foundation of China (No. 20375034) and the Novel Foundation of Jiangsu Provincial Education Department for Doctors (2005).

#### References

1. C. Wang, Y. Chen, F. Wang and X. Hu, Fabrication of nanometer-sized carbon electrodes by the controllable electrochemical deposition. *Electrochim. Acta*, 50 (2005) 5588.
2. C. Wang and X. Hu, Fabrication of nanometre-sized platinum electrodes by controllable electrochemical deposition. *Talanta*, 68 (2006)1322.
3. T. Hirschfeld, Quantum efficiency independence of the time integrated emission from a fluorescent molecule. *Appl. Opt.*, 15 (1976) 3135.
4. E. B. Shera, N. K. Seitzinger, L. M. Davis, R. A. Keller and S. A. Soper, Detection of single fluorescent molecules. *Chem. Phys. Lett.*, 174 (1990) 553.
5. F.-R.F. Fan and A. J. Bard, Electrochemical detection of single molecules. *Science*, 267 (1995) 871.
6. F.-R.F. Fan and A. J. Bard, An electrochemical coulomb staircase: detection of single electron-transfer events at nanometer electrodes. *Science*, 277 (1995) 1791.
7. M. M. Collinson and R. M. Wightman, Observation of individual chemical reactions in solution. *Science*, 268 (1995)1883.
8. J. J. Watkins, J. Y. Chen, H. S. White, Hector D. Abrun, E. Maisonhaute and C. Amatore, Zeptomole voltammetric detection and electron-transfer rate measurements using platinum electrodes of nanometer dimensions. *Anal. Chem.*, 75 (2003) 3962.
9. A. D. McFarland and R. P. V. Duyne, Single silver nanoparticles as real-time optical sensors with zeptomole sensitivity. *Nano Letters*, 3 (2003) 1057.
10. T. Matsuya, S. Tashiro, N. Hoshino, N. Shibata, Y. Nagasaki and K. Kataoka, A core-shell-type fluorescent nanosphere possessing reactive poly(ethylene glycol) tethered chains on the surface for zeptomole detection of protein in time-resolved fluorometric immunoassay. *Anal. Chem.*, 75 (2003) 6124.
11. K. Dore, S. Dubus, H. A. Ho, I. Le´vesque, M. Brunette, G. Corbeil, M. Boissinot, G. Boivin, M. G. Bergeron, D. Boudreau and M. Leclerc, Fluorescent polymeric transducer for the rapid, simple,

- and specific detection of nucleic acids at the zeptomole level. *J. Am. Chem. Soc.*, 126(2004) 4240.
12. C. J. Slevin, N. J. Gray, J. V. Macpherson, M. A. Webb and P. R. Unwin, Fabrication and characterisation of nanometre-sized platinum electrodes for voltammetric analysis and imaging. *Electrochem. Comm.*, 1 (1999) 282.
  13. F.G. Will, Hydrogen adsorption on platinum single crystal electrodes, I: isotherms and heats of adsorption. *J. Electrochem. Soc.*, 112 (1965) 451.
  14. D. F. A. Koch, and R. Woods, The electro-oxidation of acetate on platinum at low potentials. *Electrochimica Acta*, 1968, 13 (11), 2101.
  15. J. C. Huang, W. E. O'Grady and E. Yeager, The effects of cations and anions on hydrogen chemisorption at platinum. *J. Electrochem. Soc.*, 124 (1977) 1732.
  16. A. J. Bard and L.R. Faulkner, *Electrochemical Methods: Fundamentals and Applications*, 2nd. Ed., John Wiley & Sons, New York (2001).
  17. W. H. Reinmuth, Three-dimensional representation of voltammetric processes. *Anal. Chem.*, 32 (1960) 1509.
  18. J. L. Ingram and W. J. B. Fong, Frequency-dependent capacitance of microelectrode arrays and characterization of the metal | polymer interface. *J. Electroanal. Chem.*, 365 (1994) 79.
  19. M. D. Porter, T. B. Bright, D. L. Allara and C. E. D. Chidsey, Spontaneously organized molecular assemblies. 4. Structural characterization of n-alkyl thiol monolayers on gold by optical ellipsometry, infrared spectroscopy, and electrochemistry. *J. Am. Chem. Soc.*, 109 (1987) 3559.
  20. S. J. Green, J. J. Stokes, M. J. Hostetler, J. Pietron and R. W. Murray, Three-dimensional monolayers: nanometer-sized electrodes of alkanethiolate-stabilized gold cluster molecules. *J. Phys. Chem. B.*, 101 (1997) 2663.
  21. M. I. Montenegro, M. A. Queiros and J. L. Daschbach, *Microelectrodes: Theory and applications*, Kluwer Academic Press, Dordrecht, The Netherlands (1991)
  22. K. T. Kawagoe, J. A. R. Jankowski and M. Wightman, Etched carbon-fiber electrodes as amperometric detectors of catecholamine secretion from isolated biological cells. *Anal. Chem.*, 63 (1991) 1589.
  23. J. L. Conyers and Jr. H. S. White, Electrochemical characterization of electrodes with submicrometer dimensions. *Anal. Chem.*, 72 (2000) 4441.
  24. J. M. D. Rodriguez, J. A. H. Melian and J. P. Pena, Determination of the real surface area of Pt electrodes by hydrogen adsorption using cyclic voltammetry. *J. Chemical. Education*, 77 (2000) 1195.
  25. J. R. Anderson, *Structure of Metallic Catalysts*, Academic Press, London (1975)
  26. T. Biegler and D. A. Rand, Limiting oxygen coverage on platinized platinum; relevance to determination of real platinum area by hydrogen adsorption. *J. Electroanal. Chem.*, 29 (1971) 269.
  27. Y. S. Wang, S. X. Zou and Y. J. Zhang, *Modern Animal Biochemistry*, China Agriculture Science and Technology Publishing Company, Beijing (1999)